

# “Exhaustion” Physics in the Periodic Anderson Model from Iterated Perturbation Theory

N. S. Vidhyadhiraja<sup>1,2</sup>, A. N. Tahvildar-Zadeh<sup>1</sup>, M. Jarrell<sup>1</sup>, and H. R. Krishnamurthy <sup>2</sup>

<sup>1</sup> *Department of Physics, University of Cincinnati, Cincinnati, OH 45221*

<sup>2</sup> *Department of Physics, IISc, Bangalore 560012, India*

(June 9, 2024)

## Abstract

We discuss the “exhaustion” problem in the context of the Periodic Anderson Model using Iterated Perturbation theory within the Dynamical Mean Field Theory. We find that the number of electronic states available for screening near the Fermi surface have decreased, a direct confirmation of the exhaustion principle, and find evidence for suppression of the coherence temperature in the lattice case as compared to the Kondo scale in the single impurity picture. The IPT results are in qualitative agreement with recent Quantum Monte Carlo results for the same problem. Our study also elucidates the different roles played by lattice coherence and exhaustion in the suppression of the coherence temperature.

PACS. 71.28 – Narrow-band systems, heavy fermion metals: intermediate-valence solids.

PACS. 72.15Q – Scattering mechanisms and Kondo effect

*Introduction* Metallic compounds containing rare earth elements with partially filled  $f$  shells, such as  $\text{CeBe}_{13}$  or  $\text{UPt}_3$ , belong to the general category of heavy Fermion materials [1]. They are characterized by large Pauli susceptibility and specific heat coefficient as compared to ordinary metals, which indicate a huge effective electronic mass; and also by anomalous transport properties such as non-monotonic temperature dependence of the resistivity. These anomalies are usually attributed to the formation of a resonant state at the Fermi energy due to the admixture of the electronically active but highly local  $f$  orbitals with the metallic band of the host. Although these materials are normally modelled in terms of an asymmetric Periodic Anderson Model(PAM), the formation of this resonance is usually interpreted in terms of the single impurity Anderson model(SIAM) [2]. However, an impurity treatment neglects the effects of correlations between the impurity sites, lattice coherence (i.e. Bloch's theorem), and significantly, exhaustion.

The “Exhaustion” problem [3,4] originally posed by Nozières in the context of a Kondo lattice occurs when a *few* mobile electrons,  $N_{scr}$ , have to screen *many* local moments,  $N_f$ , in a metallic environment, i.e,  $N_{scr} \ll N_f$ . This situation is engendered by the fact that only the electrons within  $T_K$  (where  $T_K$  is the single impurity Kondo temperature) of the Fermi surface can effectively participate in screening the local moments. Thus the number of screening electrons can be estimated as  $N_{scr} = \rho_d(\epsilon_F)T_K$ , where  $\rho_d(\epsilon)$  is the conduction band density of states(DOS) and  $\epsilon_F$  is the Fermi level. A measure of exhaustion is the dimensionless ratio [3]

$$p = \frac{N_f}{N_{scr}} = \frac{N_f}{\rho_d(\epsilon_F)T_K}. \quad (1)$$

Nozières has argued that  $p$  is roughly the number of scattering events between a local moment and a mobile electron necessary for the mobile electron's spin to precess around a local moment by  $2\pi$  [4]. In the case  $p \gg 1$ , when the number of screening electrons is much smaller than the number of local moments to screen, magnetic screening is necessarily collective and the single impurity picture becomes invalid.

In a recent study [5,6] of the PAM using the Dynamical Mean Field Theory(DMFT), which

is exact in the  $\infty$ -dimensional limit [7], it was argued that exhaustion was responsible for the severe reduction of the Kondo scale of the PAM from that of the impurity problem with the same parameters. The issue was explored in detail [5,6] using the Quantum Monte Carlo-Maximum Entropy Method(QMC-MEM) for solving the self-consistent Anderson Impurity problem of the DMFT. The reduction of the Kondo scale and the crossover between the two scales was interpreted in terms of Nozières exhaustion principle [3], and his mapping of the model which has exhausted all available conduction band screening states onto an effective Hubbard model. Using qualitative and semi-quantitative arguments, Nozières [4] has suggested that the temperature scale  $T_c$  associated with the onset of Fermi liquid coherence in this “exhaustion” limit is suppressed compared to the Kondo temperature of the single-impurity Anderson Model (SIAM),  $T_K$ , by the factor  $p$

$$T_c \simeq T_K/p. \quad (2)$$

While the aforementioned suppression of  $T_c$  was clearly evident in the QMC simulations, no universal relation of  $T_c$  to  $T_K$  such as Eq. 2 was found.

In this work, we explore the problem of exhaustion in the context of the asymmetric PAM using Iterated Perturbation theory (IPT) [8] within the DMFT. We calculate the spectral functions and as a check on the accuracy of IPT, compare them with earlier QMC-MEM results [5,6]. We find reasonable agreement between the two. Using the spectral functions calculated for the PAM and the SIAM, we identify the “coherence temperature”,  $T_c$  and the “Kondo Temperature”,  $T_K$  respectively. We find, consistent with the “Protracted screening” picture of ref [6] and the “Collective Kondo screening” picture of Nozières [4], a suppression of  $T_c$  as compared to  $T_K$ . Furthermore, we find  $T_c$  and  $T_K$  to be related as

$$T_c = \frac{T_K}{\alpha(U, V)p_0}. \quad (3)$$

Here  $\alpha(U, V)$  is the fitting parameter and  $p_0$  is defined (similarly to Eq 1) as  $p_0 \equiv N_f/(\rho(x)T_K)$ , where  $\rho(\epsilon)$  is the bare conduction DOS and  $x$  is determined by  $n_d = 2 \int_{-\infty}^x d\epsilon \rho(\epsilon)$ . As discussed below, our calculations also help to elucidate the contributions to the suppression of  $T_c$  arising from lattice coherence effects and exhaustion.

*Model and Formalism* The PAM Hamiltonian on a  $D$ -dimensional hypercubic lattice is

$$H = \frac{-t^*}{2\sqrt{D}} \sum_{\langle ij \rangle \sigma} (d_{i\sigma}^\dagger d_{j\sigma} + H.c) + \sum_{i\sigma} (\epsilon_d d_{i\sigma}^\dagger d_{i\sigma} + \epsilon_f f_{i\sigma}^\dagger f_{i\sigma}) + V \sum_{i\sigma} (d_{i\sigma}^\dagger f_{i\sigma} + H.c) + U \sum_i n_{fi\uparrow} n_{fi\downarrow}. \quad (4)$$

In Eq. 4,  $d_{i\sigma}^{(\dagger)} (f_{i\sigma}^{(\dagger)})$  is a creation operator that creates a  $d(f)$ –electron with spin  $\sigma$  on site  $i$ ;  $d_{i\sigma} (f_{i\sigma})$  is the corresponding destruction operator. The hopping is restricted to the nearest neighbors and scaled as  $t = t^*/2\sqrt{D}$ .  $U$  is the on-site Coulomb repulsion for the localized  $f$  states,  $V$  is the hybridization between  $d$  and  $f$  states and  $\epsilon_f, \epsilon_d$  are the site energies for  $f$  and  $d$  electrons.

We work in the infinite-dimensional limit where it was shown by Metzner and Vollhardt [7] that the irreducible self-energy and the vertex functions become purely local. As a consequence, the interacting lattice model can be mapped onto a local correlated impurity coupled to an effective bath that is self-consistently determined [9]. In this infinite dimensional limit the non-interacting DOS has the Gaussian form [7]  $\rho(\epsilon) = \frac{1}{\sqrt{\pi t^*}} \exp \left[ -\frac{\epsilon^2}{t^{*2}} \right]$ . We choose our energy scale such that  $t^* = 1$ .

The local  $f$  and  $d$ -propagators for the PAM are given by

$$G_{d,loc}(\omega) = \tilde{D} \left( \omega^+ - \epsilon_d - \frac{V^2}{\alpha(\omega)} \right) \quad (5)$$

$$\text{and } G_{f,loc}(\omega) = \frac{1}{\alpha(\omega)} \left[ 1 + \frac{V^2}{\alpha(\omega)} G_{d,loc}(\omega) \right] \quad (6)$$

where  $\tilde{D}(z) \equiv \int_{-\infty}^{\infty} d\epsilon \frac{\rho(\epsilon)}{z - \epsilon}$  is the Hilbert Transform of  $\rho(\epsilon)$  and  $\alpha(\omega) \equiv \omega^+ - \epsilon_f - \Sigma(\omega^+)$  where  $\omega^+ = \omega + i0$ .

The self-consistent host is determined by the bare local propagator of the effective single-site problem as

$$\mathcal{G}^{-1} = G_{f,loc}^{-1} + \Sigma \quad (7)$$

and self-consistency is achieved through the use of Eqs. 5, 6 and the result for the self-energy for the single-site, or the impurity problem  $\Sigma \equiv \Sigma(\mathcal{G})$ .

Given a starting self-energy, we use Eqs. 5,6 and 7 to compute  $\mathcal{G}$ , and then a prescription for the effective single-impurity problem to calculate the new self-energy. This procedure is repeated until self-consistency is achieved.

We use Iterated Perturbation Theory(IPT) [8] as the prescription to calculate the self-energy for the effective impurity problem. The motivation for using this scheme is that it is semi-analytical and much easier to implement than Quantum Monte Carlo(QMC). While it has the disadvantage that it is perturbative and there is some ambiguity in extending it to finite temperatures [10], its advantages are that we obtain real-frequency data directly at zero temperature. We now briefly review this scheme.

The IPT ansatz [8] for the total self-energy is given by

$$\Sigma_{int}(\omega) = \frac{U \langle n_f \rangle}{2} + \frac{A \Sigma_2(\omega)}{[1 - B \Sigma_2(\omega)]} \quad (8)$$

where  $\Sigma_2(\omega)$  is the second order self-energy defined in terms of a modified bare local propagator  $\tilde{\mathcal{G}}^{-1} = \mathcal{G}^{-1} + \epsilon_f + \mu_0$ . The parameter  $\mu_0$  is adjusted so as to satisfy the Luttinger's theorem [11],  $\text{Im} \int_{-\infty}^0 \frac{\partial \Sigma_2(\omega)}{\partial \omega} G_{f\sigma}(\omega) d\omega = 0$ . A and B are chosen so as to reproduce the atomic limit and the high frequency behavior of the self-energy at any filling, which yields [8]

$$A \equiv \frac{n_f(2 - n_f)}{n_0(2 - n_0)}; \quad B \equiv \frac{4((1 - n_f/2)U + \epsilon_f + \mu_0)}{n_0(2 - n_0)U^2}. \quad (9)$$

Here  $n_f \equiv 2 \int_{-\infty}^0 \rho_f(\omega) d\omega$ , is the f-band filling and  $n_0$  is defined by  $n_0 \equiv 2 \int_{-\infty}^0 \rho_{\mathcal{G}}(\omega) d\omega$ , where  $\rho_f$  and  $\rho_{\mathcal{G}}$  are the spectral functions of  $G_f$  and  $\mathcal{G}$  respectively:  $\rho_f \equiv -\frac{1}{\pi} \text{Im} G_f(\omega^+)$ , and  $\rho_{\mathcal{G}} \equiv -\frac{1}{\pi} \text{Im} \mathcal{G}(\omega^+)$ ,

The conduction band filling is varied by varying  $\epsilon_d$ . We maintain an *f*-band filling close to one, i.e  $n_f \simeq 1$  by adjusting  $\epsilon_f$ . The actual value used for  $n_f$  was 0.99, and the accuracy achieved in fixing this value was  $\sim 1$  in  $10^5$ . For reasons of numerical convenience, we calculate the second-order self-energy directly for real frequencies in two steps. We first calculate the imaginary part of  $\Sigma_2$  using convolution integrals on a lorentzian frequency grid; then use Kramer's-Kronig relations to find its real part. Typically we achieve self-consistency of the Green functions within 3 to 4 iterations and the solution for  $\epsilon_f$  and  $\mu_0$  is found within 10(outer loop) iterations using a non-linear equation solving routine.

*Results* We have performed the calculations described above for various values of  $U$  and  $V$  and we present and discuss some representative results. Since IPT is a perturbative technique, we have checked its accuracy by comparing it with the earlier QMC-MEM [5,6] results for  $U = 1.5$  and  $V = 0.6$ .

Fig. 1 shows the  $f$ -spectral function for IPT at zero temperature and QMC-MEM at  $T = 0.025$  for three conduction band fillings namely  $n_d = 0.4, 0.6$  and  $0.8$ . Both the QMC-MEM and IPT results share some common features. For small  $n_d$  a single narrow Kondo peak is centered at the Fermi energy  $\omega = 0$ ; however as  $n_d \rightarrow 1$ , the peak broadens and splits in two, with both peaks shifted from the Fermi energy. Apparently, the latter is a remnant of the insulating gap found when  $n_f = n_d = 1$ .

We see that the IPT results match very well with QMC-MEM for  $n_d = 0.8$ , but as  $n_d$  is decreased the deviation increases. The difference in the width of the Kondo resonance between IPT and QMC in the low  $n_d$  or the exhaustion limit could be due to two factors:(1)the calculations for the latter were carried out at higher temperatures which would lead to temperature broadening,(2) IPT is perturbative in  $U$  while the impurity Kondo energy scale,  $T_K$  is exponential in  $U$ . Thus, IPT could become less accurate for small  $n_d$  since the effective  $\Gamma(0)$  is decreasing as  $n_d$  decreases(see below).

In the QMC-MEM work [5,6], the SIAM Kondo scales and the PAM coherence scales were identified from the  $T \rightarrow 0$  limit of the appropriate impurity spin susceptibility as  $\chi_{imp}^{-1}(T \rightarrow 0)$ (using the bare impurity for the SIAM and the self-consistently embedded impurity for the PAM). Since IPT is not a conserving approximation, there is no unique way of calculating the susceptibility. So we do not use the susceptibility to measure  $T_c$ . Instead, as an alternate measure of the Kondo and coherence scales, we calculate the Full Width at Half Maximum(FWHM) of the Kondo resonance in the  $f$ -spectral function for the SIAM and PAM and identify these with  $T_K$  and  $T_c$  respectively. We present our results for these in Fig. 2 for  $U = 1.5$  and  $V = 0.6$ .  $T_c$  is seen to be much suppressed as compared to  $T_K$ , corroborating Nozières' arguments [3,4] and the QMC-MEM results [6,5].

As mentioned earlier, we find that  $T_c$  and  $T_K$  are related according to Eq. 3. We have

checked this for four sets of parameters and we show the values of  $\alpha$  and  $\sigma$ (standard deviation) in Table. I for each of these sets.

More direct evidence for exhaustion is seen in the dip near the Fermi level in the effective hybridization The effective hybridization of the self-consistent single impurity problem is given by  $\Gamma(\omega) = \mathbf{Im}\mathcal{G}^{-1} = \mathbf{Im}\left(G_{f,loc}^{-1} + \Sigma\right)$ . It is shown in Fig. 3 as calculated within QMC-MEM [5,6] and IPT. Again the agreement is good.

Exhaustion can generally be understood as referring to the decrease in the number of  $d$  electron states near the Fermi surface due to the formation of Kondo singlet states on the localized  $f$ -orbital sites. Hence the dip in  $\Gamma(\omega)$  for  $\omega \approx 0$  seen in Fig 3 can be interpreted as a confirmation of Nozières argument. We also compare the Hartree  $\Gamma(\omega)$  [12] with the PAM-IPT  $\Gamma(\omega)$  and the SIAM  $\Gamma(\omega)$ ( $\equiv \pi V^2 \rho(\omega + x)$  where  $\rho$  and  $x$  are defined below Eq. 3) in Fig 4(a). The Hartree hybridization is rather flat near the Fermi level while the PAM-IPT hybridization has a strong energy dependence reflected by the dip. While the Hartree  $\Gamma$ , which we interpret as containing the effects of lattice coherence but not of exhaustion, is also strongly suppressed compared to SIAM  $\Gamma$ , and has almost the same value as the PAM-IPT  $\Gamma$  near the Fermi level, the FWHM of the Kondo resonance of the PAM-IPT spectral function shown in Fig 4(b) is much smaller compared to that of the Hartree spectral function, which in turn is much smaller compared to the FWHM of the SIAM spectral function for the same parameters. This suggests that, exhaustion, leading to a strongly energy dependent suppression of  $\Gamma(\omega)$ , plays a crucial role in the suppression of  $T_c$  with respect to  $T_K$ .

To further elucidate the roles of exhaustion and lattice coherence, we have also studied a case complementary to the exhaustion limit, i.e,  $N_{scr} \gg N_f$ . As we decrease  $N_f$  keeping  $n_d$  fixed, the number of local moments to screen decreases. So we expect and do find, an increase in the corresponding energy scale,  $T_c$ . We also find that the dip in the hybridization near the Fermi level observed in the exhaustion limit is absent in this case, and that ,the Hartree and the full  $\Gamma$ , although still suppressed compared to the SIAM  $\Gamma$ , are almost identical and have a weak energy dependence near the Fermi level. The details will be presented elsewhere.

*Conclusions* We have studied the “exhaustion” problem in the context of the asymmetric PAM in the limit of infinite dimensions within IPT. Taking the FWHM of the Kondo resonance in  $\rho_f(\omega)$  as a measure of the (SIAM Kondo and PAM coherence) temperature scales, we find that the coherence temperature,  $T_c$  in the PAM is much suppressed as compared to the Kondo temperature,  $T_K$  for the SIAM. Furthermore, we find that  $T_c$  and  $T_K$  are related according to Eq. 3.

Our study also elucidates the different roles played by lattice coherence and exhaustion effects. Whereas lattice coherence effects give rise to a general but smooth suppression of the hybridization, it is exhaustion which gives rise to the strong energy dependent suppression of the effective hybridization near the Fermi level. This contributes crucially to the difference between  $T_c$  and  $T_K$ . This can be interpreted as a direct confirmation of Nozières exhaustion principle.

Finally, We find quantitative agreement of the DOS and  $\Gamma(\omega)$  between IPT and QMC-MEM results for  $n_d$  close to half-filling and qualitative agreement for low  $n_d$ . Thus, IPT captures the essential features of lattice exhaustion, at least for moderate values of  $U$ . Together, these results suggest that IPT should be a useful method for incorporating moderate correlation effects into *ab initio* calculations of Heavy Fermion materials [14].

It is a pleasure to acknowledge discussions with A. Chattopadhyay, J. Freericks, D. Hess, M. Hettler and Th. Pruschke. This work was supported by NSF grants DMR-9704021 and DMR-9357199, and the Ohio Board of Regents Research Challenge Award(N. S. V and H. R. K.).

## REFERENCES

- [1] For reviews, see N. Grewe and F. Steglich, *Handbook on the Physics and Chemistry of Rare Earths*, Eds. K.A. Gschneidner, Jr. and L.L. Eyring (Elsevier, Amsterdam, 1991) Vol. 14, P. 343; D. W. Hess, P. S. Riseborough, J. L. Smith, *Encyclopedia of Applied Physics* Eds. G. L. Trigg (VCH Publishers Inc., NY), Vol.7 (1993) p. 435.
- [2] L. H. Tjeng *et. al.*, Phys. Rev. Lett. **71**, 1419 (1993), see also M. Garnier *et. al.*, Phys. Rev. Lett., **78**, 4127 (1997)
- [3] P. Nozières, Ann. Phys. Fr. **10**, 19, 1985
- [4] P. Nozières, Eur. Phys. J. B **6**, 447, 1998
- [5] A. N. Tahvildar-Zadeh, M. Jarrell and J.K. Freericks, Phys. Rev. Lett. **80**, p5168, (1998).
- [6] A. N. Tahvildar-Zadeh, M. Jarrell and J. K. Freericks, Phys. Rev. B **55**, R3332 (1997)
- [7] W. Metzner and D. Vollhardt, Phys. Rev. Lett. **62**, 324 (1989); A. Georges, G. Kotliar, W. Krauth, and M. J. Rozenberg, Rev. Mod. Phys. **68**, 13 (1996); Th. Pruschke, M. Jarrell and J. K. Freericks, Adv. in Phys. **42**, 187(1995)
- [8] H. Kajueter and G. Kotliar, Phys. Rev. Lett. **77**, 131 (1996)
- [9] U. Brandt and C. Mielsch, Z. Phys. B **75**, 365 (1989); **79**, 295 (1990); **82**, 37 (1991); V. Janiš, *ibid.* **83**, 227 (1991); C. Kim, Y. Kuramoto, and T. Kasuya, J. Phys. Soc. Jpn. **59**, 2414 (1990); V. Janiš and D. Vollhardt, Int. J. Mod. Phys. B **6**, 713 (1992); M. Jarrell, Phys. Rev. Lett. **69**, 168 (1992); A. Georges and G. Kotliar, Phys. Rev. B **45**, 6479 (1992)
- [10] P. Majumdar, H. R. Krishnamurthy cond-mat/9512151
- [11] J. M. Luttinger, Phys. Rev. **119**, 1153 (1960); *ibid.*, **121**, 942 (1961)
- [12] If we calculate  $\epsilon_f$  and  $\epsilon_d$  for the PAM, keeping only the Hartree term for the self-energy, with the constraint that the  $n_f$  and  $n_d$  values should be the same as for the

PAM-IPT, then the hybridization calculated with these  $\epsilon_f$  and  $\epsilon_d$  is being called the Hartree hybridization.

[13] T.M. Rice and K. Ueda, Phys. Rev. B **34**, 6420 (1986); M. Jarrell, Phys. Rev. B. **51**, 7429-40 (15, March 1995).

[14] M. M. Steiner, R. C. Albers, and L. J. Sham, Phys. Rev. Lett. **72**, 2923 (1994), V. I. Animosov *et al*, cond-mat/9704231

#### TABLES

U	1.5	1.5	2.0	2.0
V	0.5	0.6	0.5	0.6
$\alpha$	1.4	4.06	0.75	2.55
$\sigma$	0.0041	0.0037	0.0050	0.0033

TABLE I. Table showing the values of  $\alpha$  and  $\sigma$  for four sets of  $U$  and  $V$ .

#### FIGURES

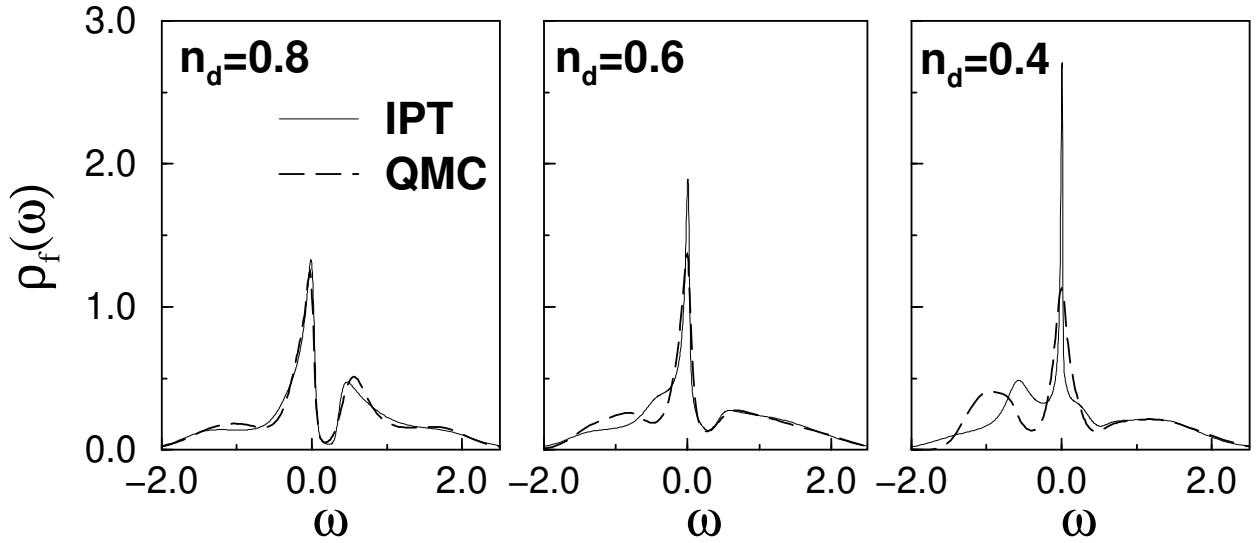


FIG. 1. Comparison of the  $f$  density of states obtained from IPT and QMC for three fillings of the conduction band,  $n_d = 0.4, 0.6, 0.8$ , with  $n_f \simeq 1$ , for  $U = 1.5$ ,  $V = 0.6$ .  $T = 0$  for IPT and  $T = 0.025$  for QMC. The agreement is quite good for  $d$ -fillings close to one.

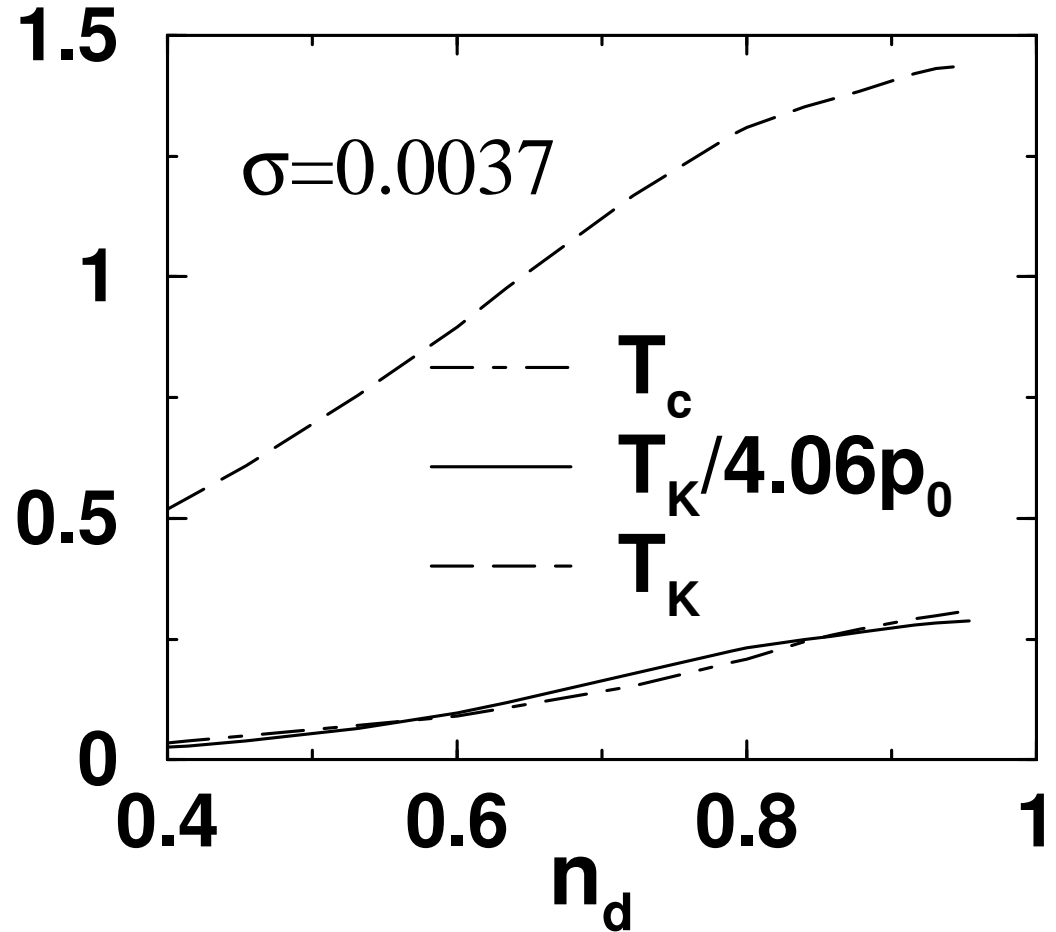


FIG. 2. The full width at half maximum for the Kondo resonance in the  $f$ -spectral function ,(which is taken as a measure of “ $T_K$ ” for the SIAM and “ $T_c$ ” for the PAM ) for  $U = 1.5$  and  $V = 0.6$  as a function of the conduction band filling. The solid line shows  $T_K/\alpha(U,V)p_0$ .  $\sigma$  is the standard deviation for fitting the above relation to  $T_c$  with  $\alpha$  as the adjustable parameter.

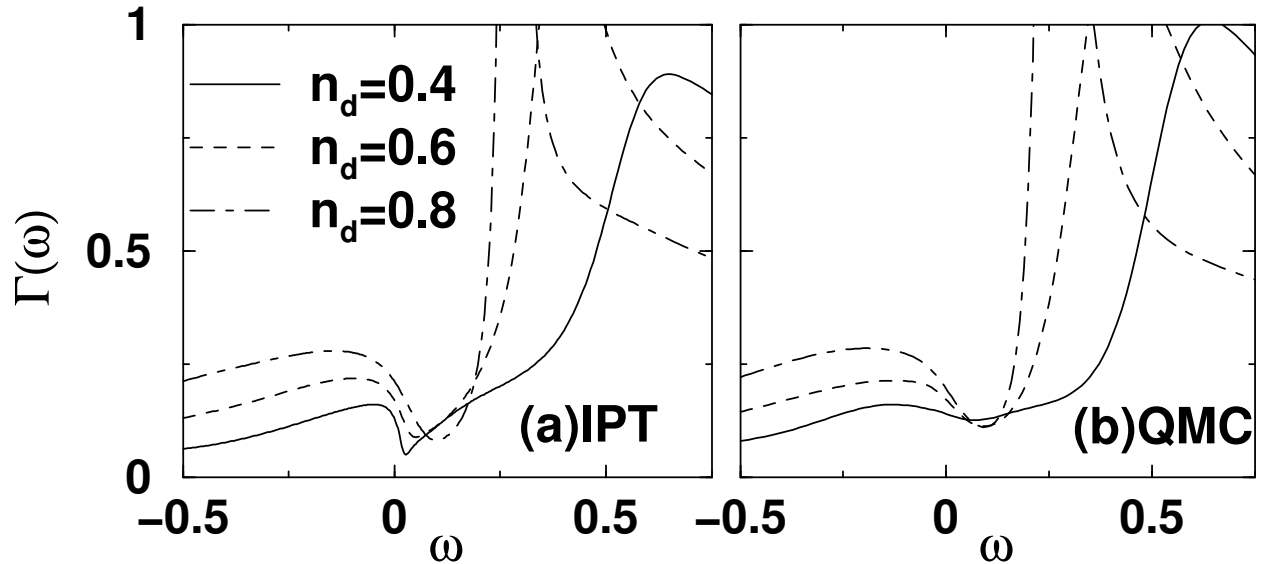


FIG. 3. The effective hybridization within (a) IPT and (b) QMC–MEM for the same parameters as Fig. 1 showing the decrease in the number of states available for Kondo screening near the Fermi level.

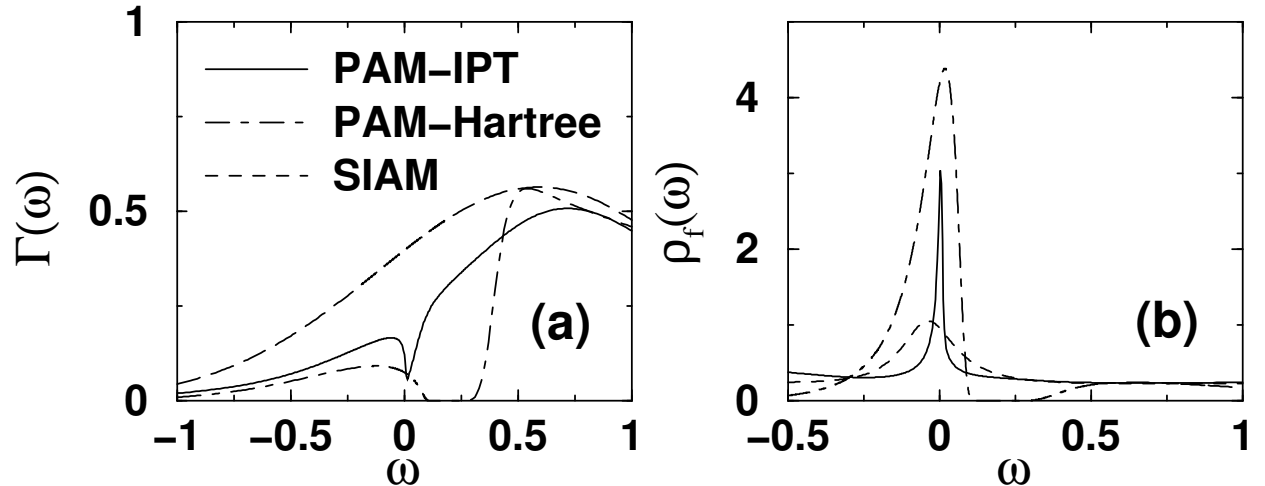


FIG. 4. (a) The PAM–IPT , the PAM–Hartree and the SIAM hybridization showing the effects of lattice coherence and exhaustion for  $U = 1.5, V = 0.5$ , and  $n_d = 0.4$ . Near the Fermi level, the PAM–IPT  $\Gamma$  has a dip reflecting a strong energy dependence. Both the PAM–IPT and Hartree  $\Gamma$  are seen to be much suppressed compared to the SIAM  $\Gamma$  . (b) The corresponding  $f$ –spectral functions are shown for the same parameters as (a). The Kondo peak broadens for the three cases progressively.